

# 6C radio galaxies at $z \sim 1$ : The influence of radio power on the alignment effect

Katherine J. Inskip<sup>a</sup> Philip N. Best<sup>b</sup> Malcolm S. Longair<sup>a</sup>

<sup>a</sup>*Astrophysics Group, Cavendish Laboratory*

<sup>b</sup>*IfA, Edinburgh*

---

## Abstract

Powerful radio galaxies often display enhanced optical/UV continuum emission and extended emission line regions, elongated and aligned with the radio jet axis. The expansion of the radio source strongly affects the gas clouds in the surrounding IGM, and the kinematic and ionization properties of the extended emission line regions display considerable variation over the lifetime of individual sources, as well as with cosmic epoch. We present the results of deep rest-frame UV and optical imaging and UV spectroscopy of high redshift 6C radio galaxies. The interdependence of the host galaxy and radio source properties are discussed, considering: (i) the relative contribution of shocks associated with the expanding radio source to the observed emission line gas kinematics, and their effect on the ionization state of the gas; (ii) the similarities and differences between the morphologies of the host galaxies and aligned emission for a range of radio source powers; and (iii) the influence of radio power on the strength of the observed alignment effect.

*Key words:* galaxies: active — galaxies: evolution — radio continuum : galaxies

---

## 1 Introduction

At high redshifts, radio galaxies are observed to be surrounded by extended regions of UV/optical continuum emission, often well aligned with the radio source axis. This *Alignment Effect* has been well studied in the 3CR sample. At  $z \sim 1$ , the aligned structures are typically brighter and more extensive than at lower redshifts, and more closely aligned with the radio emission. A number of different emission mechanisms have been proposed in order to explain the alignment effect; the most likely models include scattering of the UV continuum emission from the AGN (1), jet-induced star formation (2) and nebular continuum emission (3). Additionally, these distant radio galaxies also display extended regions of line emission. One problem with studies of 3CR radio galaxies is that the radio power of these sources increases with redshift,

leading to a degeneracy between radio power and  $z$ . The stronger alignment effect seen in the more powerful higher redshift objects indicates that the properties of the aligned emission regions are likely to be closely linked with those of the radio source. It is therefore important that the effects of the radio source properties (size, age and power) on the alignment effect are fully understood. The 6C sample studied in combination with the more powerful 3CR radio galaxies at the same redshift provides a population of radio galaxies ideally suited for this investigation, as this enables the  $P - z$  degeneracy to be broken. We have carried out a program of multiwavelength imaging and spectroscopic observations of a complete subsample of 11 6C radio sources (4) with flux densities of  $2.0 \text{ Jy} < S_{151} < 3.93 \text{ Jy}$ ,  $08^h20^m < RA < 13^h01^m$ ,  $34^\circ < \delta < 40^\circ$  and  $0.85 < z < 1.5$ . The 6C galaxies are  $\sim 6$  times less powerful radio sources than the 3CR subsample previously studied by Best et al (5; 6); the sample membership is illustrated in Fig. 1.

## 2 The emission line gas

Deep spectroscopic observations have been carried out for many of the 6C and 3CR radio galaxies in the redshift range  $0.85 < z < 1.25$  (6; 7). Many useful results have been obtained from this data, including the variation in the ionization state and gas kinematics (Fig. 2) with radio power, radio size and redshift. A statistical analysis of this data shows that the smaller and more powerful radio sources display more extreme kinematics. The spectra of these small sources ( $D_{rad} < 120 \text{ kpc}$ ) are well explained by significant levels of shock ionization in addition to photoionization by the obscured AGN, unlike the larger sources for which the emission line ratios can be explained simply by AGN photoionization.

## 3 Morphological properties

The imaging observations (10) of the 6C galaxies (Fig. 3) have also produced a number of interesting results. The UKIRT observations are dominated by the emission from the old stellar populations and reveal elliptical host galaxies, whereas the HST observations show a variety of morphologies, often with considerable extended emission aligned with the radio source axis. These structures are similar to those observed for the 3CR sources (5) at  $z \sim 1$  (Fig. 4), and include arcs and filamentary structures, diffuse emission and bright knots of emission. Typically, each source displays several of these different features, although some sources (e.g. 6C1019+39, 3C65) appear completely passive, with little sign of any extended aligned structures. Additionally, several sources in the sample appear to be interacting with close companions.

Despite the similarities, there are also notable differences in the aligned struc-

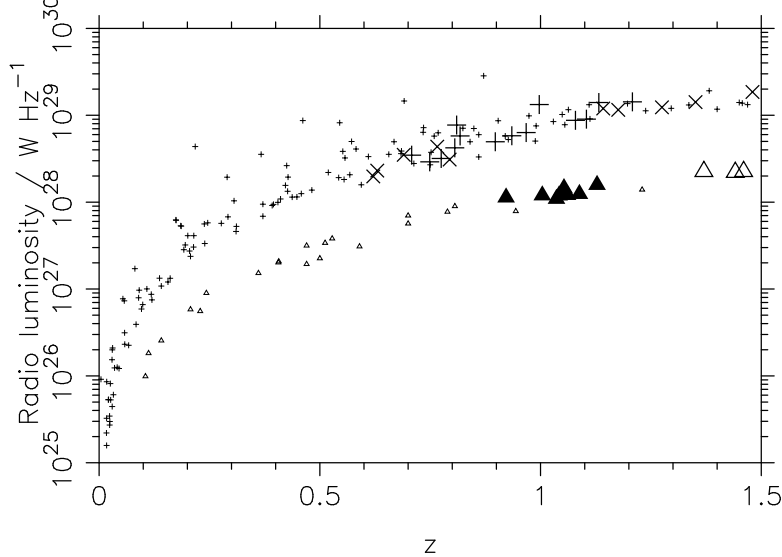


Fig. 1.  $P$ - $z$  diagram illustrating the full 3CR and 6CE samples (small symbols), and the  $z \sim 1$  subsamples (large symbols). The 6C sources are denoted by triangles, and the 3CR sources by '+' and 'x'. (Deep spectra have been obtained for the galaxies denoted by a filled triangle or '+'.)

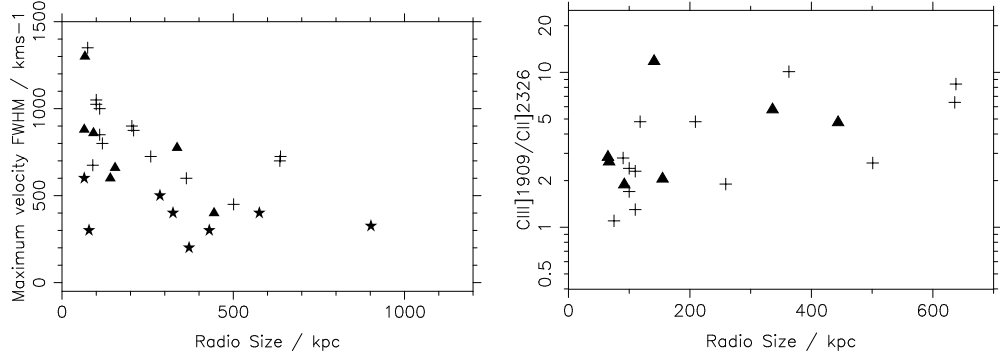


Fig. 2. (a – left) The variation of the [OII] FWHM with radio size for the  $z \sim 1$  6C and 3CR galaxies (symbols as in Fig. 1), and a sample of low- $z$  3CR sources (8; 9) (denoted by stars) matched in radio power to the 6C sources. Partial rank statistics show that FWHM is independently correlated with radio power, redshift and radio size at significance levels of +93%, +94% and –99% respectively. (b – right) The CIII]1909/CII]2326 emission line ratio vs. radio size for the same sources; these data are correlated with radio size at a significance level of > 99%. For both subsamples, the smaller radio galaxies exist in a lower ionization state.

tures observed in each sample. Whilst the smaller 3CR sources display a clear tendency to have more extensive, luminous and knotty aligned structures, this is not obvious for the 6C galaxies at the same redshifts. The aligned emission surrounding the 6C galaxies is usually also less extensive. Additionally, the extended strings of very bright knots of emission seen around the smaller 3CR radio galaxies are generally not observed in the 6C sample.

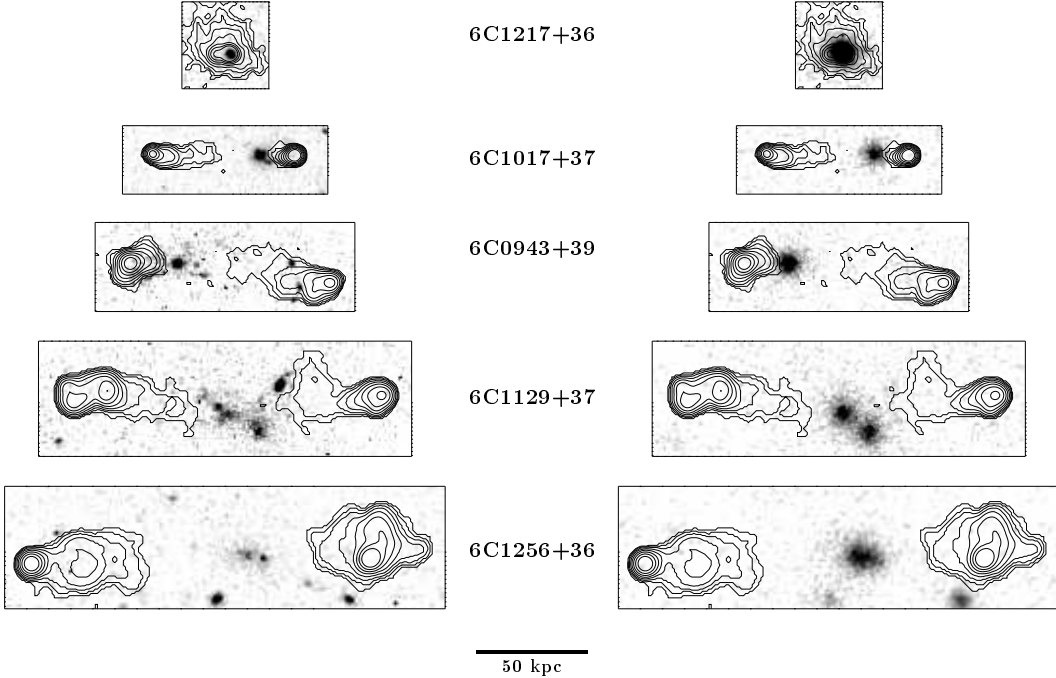


Fig. 3. HST and UKIRT images of the five smallest of 7 6C radio galaxies in the redshift range  $1 < z < 1.3$ . Contours represent the 5GHz VLA observations.

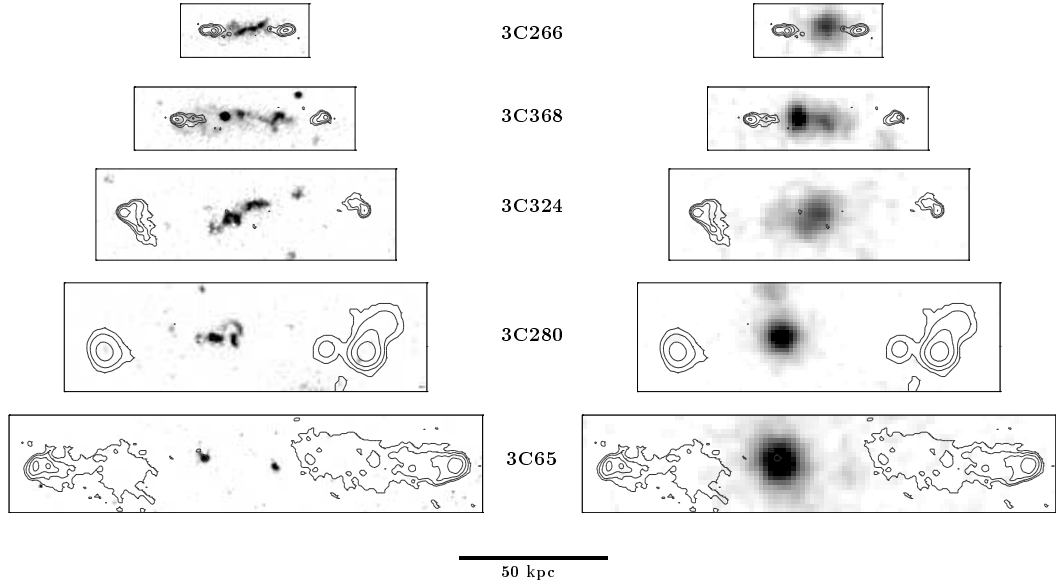


Fig. 4. HST and UKIRT images of the five smallest of 8 3CR radio galaxies in the redshift range  $1 < z < 1.3$ . Contours represent the 8GHz VLA observations.

#### 4 The alignment effect

The power of a radio source clearly plays a role in producing the observed properties of the alignment effect. In order to investigate the effects of radio power more fully, we have quantified the alignment effect in terms of the physical extent of the aligned emission, and the degree to which it is aligned with the axis of the radio source. The *Alignment Strength* is given by  $a_s =$

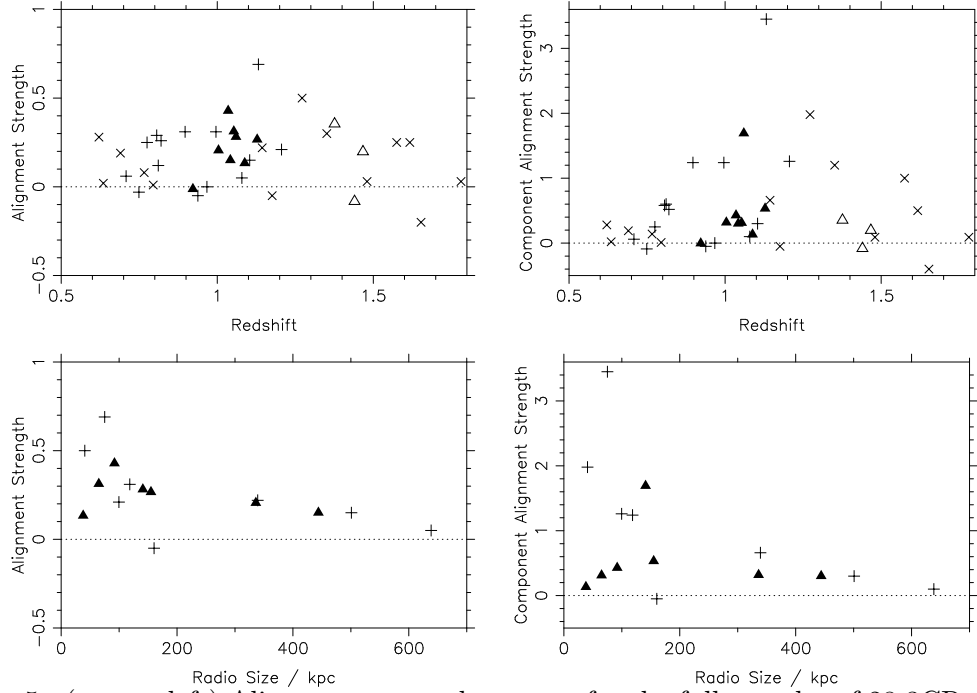


Fig. 5. (a - top left) Alignment strength  $a_s$  vs.  $z$  for the full samples of 28 3CR and 11 6C galaxies. (b - top right) Component alignment strength  $a_c$  vs.  $z$  for the same data as in (a). (c - bottom left)  $a_s$  vs. radio size for the 6C and 3CR radio galaxies in the redshift range  $1.0 < z < 1.3$ . (d - bottom right)  $a_c$  vs. radio size, for the same data as in (c). Symbols as in Fig. 1.

$\epsilon(1 - \Delta PA/45)$ , where  $\epsilon$  is the ellipticity of the aligned emission, and  $\Delta PA$  is the difference in position angle between the radio and rest-frame UV emission. The “knottiness” of the aligned structures can be considered in terms of the *Component Alignment Strength*, defined as  $a_c = N_c a_s$ , where  $N_c$  represents the number of discrete bright components of emission. Figure 5 displays the variation in  $a_s$  and  $a_c$  with redshift and radio size for the galaxies in both samples. Both  $a_s$  and  $a_c$  increase with redshift out to  $z = 1.1$ , reflecting the increasing importance of the alignment effect at higher redshifts. A similar trend is also observed in the case of the galaxy colours, which become bluer with increasing  $z$  for both samples. The decrease in alignment strengths at high redshifts is due to the lower sensitivity of these observations.

In order to investigate the effects of radio size on the alignment strength whilst avoiding confusion with variations with redshift, only sources within the redshift range  $1 < z < 1.3$  are considered. Overall, both alignment strength parameters generally decrease with radio size; this trend is most obvious for the component alignment strength. Considering the individual samples,  $a_s$  and  $a_c$  clearly decrease with radio size for the 3CR sources. However, whilst the variation in  $a_s$  is almost identical for the 6C sources, the component alignment strengths of the 6C sources are very much weaker, and a clear decrease in  $a_c$  with radio size such as that seen in the case of the more powerful 3CR radio

sources is not observed. A large value of the component alignment strength, as seen for the smaller 3CR galaxies, denotes that the source has a large number of bright knots of emission, well aligned with the radio source structure. This result confirms the observations that such features are present in the smaller 3CR sources, but not in the less powerful 6C radio sources at the same redshift. This is the first obvious effect of the power of the radio source on the properties of the aligned emission.

## 5 Conclusions

From our study of 6C and 3CR sources at  $z \sim 1$ , we find that although the size/age of the radio source has the greatest effect on the emission line gas kinematics and ionization state, radio power is also an important parameter. For the properties of the continuum emission surrounding these sources, radio size and  $z$  are again the most influential parameters. The alignment effect is more extreme at higher redshifts, and for the smaller radio sources in the sample; this result is also reflected in the variation of the galaxy colours. Radio power does not influence alignment strength, and very little difference is seen between the two  $z \sim 1$  samples, except in the case of the smaller 3CR sources which display more extreme morphologies and noticeably higher component alignment strengths. It is clear that different emission mechanisms dominate under different conditions, suggesting that the importance of the mechanism which produces the bright strings of knots seen in the 3CR sample is directly linked to radio power.

## References

- [1] Cimatti A., di Serego Alighieri S., Fosbury R. A. E., Salvati M., Taylor D., 1993, MNRAS, 264, 421
- [2] Chambers K. C., Miley G. K., van Breugel W. J. M., 1987, Nat, 329, 604
- [3] Osterbrock D. E., 1989, *Astrophysics of Gaseous Nebulae and Active Galactic Nuclei*, Mill Valley: University Science Books
- [4] Best P. N., Eales S. A., Longair M. S., Rawlings S., Röttgering H. J. A., 1999, MNRAS, 303, 616
- [5] Best P. N., Longair M. S., Röttgering H. J. A., 1997, MNRAS, 292, 758
- [6] Best P. N., Röttgering H. J. A., Longair M. S., 2000, MNRAS, 311, 1
- [7] Inskip K. J., Best P. N., Rawlings S., Longair M. S., Cotter G., Röttgering H. J. A., Eales S. A., 2002, MNRAS, 337, 1381
- [8] Baum S. A., McCarthy P. J., 2000, ApJ, 119, 2634
- [9] Inskip K. J., Best P. N., Röttgering H. J. A., Rawlings S., Cotter G., Longair M. S., 2002, MNRAS, 337, 1407
- [10] Inskip K. J., 2002, PhD thesis, Cambridge University